Conductance and gating effects at sputtered oxide interfaces

Yin, C.

Citation

Yin, C. (2019, July 3). *Conductance and gating effects at sputtered oxide interfaces*. *Casimir PhD Series*. Retrieved from https://hdl.handle.net/1887/74527

Version: Not Applicable (or Unknown)

License: Leiden University Non-exclusive license

Downloaded from: https://hdl.handle.net/1887/74527

Note: To cite this publication please use the final published version (if applicable).

Cover Page

Universiteit Leiden

The handle http://hdl.handle.net/1887/74527 holds various files of this Leiden University dissertation.

Author: Yin, C.
Title: Conductance and gating effects at sputtered oxide interfaces
Issue Date: 2019-07-03

3

Controlling the interfacial conductance in $LaAlO_3/SrTiO_3$ in 90° off-axis sputter deposition

In this Chapter, we mainly study the fabrication of conducting interfaces between $LaAlO_3$ and $SrTiO_3$ by 90° *off-axis sputtering in an Ar atmosphere. At a growth pressure of* 0.04 mbar *the interface is metallic, with a carrier density of the order of* $1 \times 10^{13}\,\mathrm{cm}^{-2}$ *at* 3 K. *By increasing the growth pressure, we observe an increase of the out-of-plane lattice constants of the $LaAlO_3$ films while the in-plane lattice constants do not change. Also, the low-temperature sheet resistance increases with increasing growth pressure, leading to an insulating interface when the growth pressure reaches* 0.10 mbar. *We attribute the structural variations to an increase of the La/Al ratio, which also explains the transition from metallic behavior to insulating behavior of the interfaces. Our research shows that the control which is furnished by the Ar pressure makes sputtering as versatile a process as pulsed laser deposition, and emphasizes the key role of the cation stoichiometry of $LaAlO_3$ in the formation of the conducting interface.*

Parts of this Chapter have been published as C. Yin, D. Krishnan, N. Gauquelin, J. Verbeeck, and J. Aarts, *Controlling the interfacial conductance in $LaAlO_3/SrTiO_3$ in* 90° *off-axis sputter deposition*, Physical Review Materials **3**, 034002 (2019) [116].

3.1. Introduction

The discovery of a high-mobility conductive interface between $LaAlO_3$ and $SrTiO_3$ has given rise to numerous investigations since 2004 [9]. This two-dimensional electron system (2DES) exhibits many intriguing physical properties, including superconductivity [6], signatures of magnetism [7, 10–12, 15], and multiple electric field tunable effects [18, 26, 30, 63, 71, 72]. However, after 15 years of intensive study, the origin of the 2DES in still under debate. Proposed explanations basically fall into two classes, namely intrinsic charge transfer and extrinsic defects mechanisms. The intrinsic mechanism considers polar discontinuity between the polar $LaAlO_3$ and the nonpolar $SrTiO_3$, which leads to a charge transfer above a critical thickness of $LaAlO_3$ films [23]. The extrinsic mechanisms involve defects formed at the interface during the film deposition process, such as oxygen vacancies in the $SrTiO_3$ substrate [41–43] and cation intermixing at the interface [32, 50].

Pulsed laser deposition (PLD) is by far the most commonly used growth method to prepare $LaAlO_3/SrTiO_3$ interfaces. During the PLD process, high-energy particle bombardments could introduce the above defects at the interface, which makes it difficult to understand the roles of the intrinsic and extrinsic mechanisms [32].

Alternative growth techniques bring new insights here. Warusawithana *et al.* [59] have grown $LaAlO_3$ films by molecular beam epitaxy (MBE). The interesting outcome is that interfacial conductance can only be observed in Al-rich samples (La/Al $\leqslant$ 0.97). Their further density functional theory (DFT) calculations demonstrate the different roles of defects in the charge transfer mechanism. In Al-rich samples, Al can fill La vacancies without changing the net charge of the (001) planes. The electronic reconstruction can still transfer electrons to the interface. In La-rich samples, however, La can not substitute for Al, resulting in the formation of Al_2O_3-vacancy complexes which prohibits the charge transfer.

Sputter deposition has also been used. High-pressure (typically 1 mbar) on axis sputtering in pure oxygen yielded $LaAlO_3$ films with a La/Al ratio of 1.07, and insulating interfaces [57]. Podkaminer *et al.* [103] have shown that 90° off-axis sputtering in pure Ar is capable of growing epitaxial and smooth $LaAlO_3$ films with conductive interfaces.

In this Chapter, we first show the optimization of growth parameters for depositing high quality epitaxial $LaAlO_3$ films by 90° off-axis sputtering. We use Ar as sputter gas but we also investigate the effect of mixing in oxygen. Then we demonstrate the tuning of La/Al ratio in $LaAlO_3$ films by varying sputtering pressures. As a consequence, we observe strong but controlled variations in the interfacial conductivity.

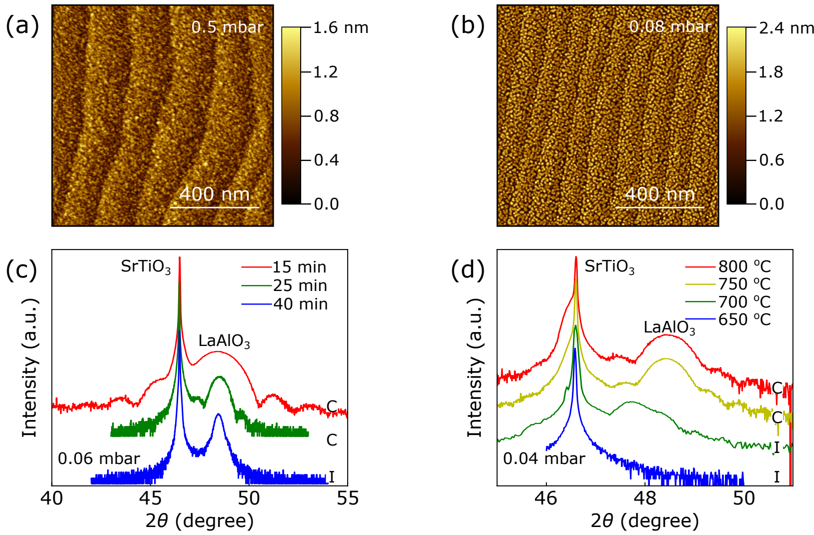

Figure 3.1: Optimization of growth parameters. (a) AFM image of a insulating sample grown by a sintered $LaAlO_3$ target. The sample was grown at 800 °C and 0.5 mbar. A single crystal $LaAlO_3$ wafer was later used as the sputtering target. (b) AFM image of an insulating sample grown in a mixture of Ar and O_2. The sample was grown at 800 °C with a total pressure of 0.08 mbar and an O_2 partial pressure of 2.0×10^{-3} mbar. (c) The θ-2θ scans for samples grown at 800 °C and 0.06 mbar for various times. "C" and "I" represent conductive and insulating, respectively. (d) The θ-2θ scans for samples grown at various temperatures and 0.06 mbar for 25 min.

3.2. Optimization of growth parameters

The main control parameters for sputter deposition include RF power, growth temperature and sputtering pressure. In Ref. [103], Podkaminer and co-workers used a single crystal $LaAlO_3$ wafer as the sputtering target. Conductive $LaAlO_3/SrTiO_3$ interfaces were prepared at a RF power of 50 W, a growth temperature of 780 °C and an Ar pressure of 0.27 mbar. Before deposition, the target was pre-sputtered for at least 15 min to stabilize a background oxygen partial pressure produced from the target. After deposition, the samples were annealed for 1 h in 400 mbar O_2 at 600 °C to remove oxygen vacancies formed in the $SrTiO_3$ substrates. In our experiments, we follow this procedure and keep the RF power constant at 50 W. In this section, we show the roles of different growth parameters in the formation of conductive interfaces.

Sputtering target

We first used a 2-inch commercial $LaAlO_3$ target (99.9 %, K. J. Lesker), which was fabricated by sintering. The growth temperature and Ar pressure were 800 °C and 0.27 mbar, respectively. The sample surface was very rough and the interface was insulating. The

surface roughness was greatly reduced by increasing the Ar pressure. Fig. 3.1(a) shows the AFM image of a sample grown at 0.5 mbar, however the interface was still insulating. There are two problems in using a sintered target. First, the DC bias on the target is relatively high (typically ~ -175 V). The ejected high-energy atoms still cause a severe back sputtering at lower Ar pressures. Although the surface morphology can be improved by increasing the Ar pressure, the enhanced scattering of light Al atoms may result in La-rich films [54, 57]. Second, the sintered target probably produces too much atomic oxygen during sputtering, which is due to that oxygen diffuses out along grain boundaries. Therefore, we later changed to a 2-inch single crystal $LaAlO_3$ wafer (MTI Corporation) as the sputtering target. The DC bias was effectively lowered (typically ~ -85 V) and conductive $LaAlO_3/SrTiO_3$ interfaces could be formed at a growth temperature of 800 °C and Ar pressures ranging from 0.04 to 0.08 mbar.

Oxygen in sputtering gas

Podkaminer *et al.* [103] have obtained insulating $LaAlO_3/SrTiO_3$ interfaces using a mixed sputtering gas (O_2:Ar = 3:4). We tried to mix Ar with a much smaller amount of O_2, ranging from 0.3 % to 4.2 %. The corresponding oxygen partial pressures (P_{O_2}) are between 1.6×10^{-4} and 4.5×10^{-3} mbar, which are similar to the typical growth pressures used in PLD [10]. However, we observed grainy surfaces and insulating interfaces in all of the samples. Detailed information can be found in Ref. [117]. Fig. 3.1(b) shows the AFM image of a sample grown at 800 °C with a total pressure of 0.08 mbar and a P_{O_2} of 2.0×10^{-3} mbar. We conclude that conductive $LaAlO_3/SrTiO_3$ interfaces can only be obtained by growing $LaAlO_3$ films in pure Ar.

Post oxygen annealing

Since the samples are grown in a reducing atmosphere, a large amount of oxygen vacancies will form in the $SrTiO_3$ substrate, making the $SrTiO_3$ bulk highly conductive [40]. Therefore, *in situ* oxygen annealing is essential to remove the oxygen vacancies in $SrTiO_3$. The annealing treatment is usually performed at an O_2 pressure of several hundreds of millibar [45, 46, 103]. However, this is practically impossible due to the limitations of our experimental setup. The chamber volume is $\sim$ 200 L, but the maximum oxygen flow is only 100 sccm. Therefore, it takes several tens of hours to reach the desired pressures. In our experiments, the oxygen annealing is performed at 1 mbar. We prepared two testing samples to check the effectiveness of our annealing treatment. One sample was a bare $SrTiO_3$ substrate heated up to 800 °C without film deposition. The other was an amorphous $LaAlO_3/SrTiO_3$ sample grown at room temperature and 0.08 mbar. Both samples were highly conductive, which indicates the presence of oxygen vacancies [36, 40, 45, 46].

The samples were then annealed for 1 h in 1 mbar O_2 at 600 °C and were found to be insulating.

Film thickness

Liu *et al.* [118] have shown that epitaxial strain plays an important role in controlling the conductivity at the $LaAlO_3/SrTiO_3$ interface. We deposited three samples at 800 °C and 0.06 mbar for various times. The θ-2θ scans are shown in Fig. 3.1(c). The interference fringes can be observed for the samples grown for 15 min (~ 16 uc) and 25 min (~ 27 uc) and both samples are conductive. For the sample grown for 40 min, the $LaAlO_3$ diffraction peak shifts slightly to lower angle and the interference fringes are no longer visible, indicating a relaxation of the $LaAlO_3$ layer. The sample is insulating.

Growth temperature

Caviglia *et al.* [30] fabricated high-mobility samples by depositing $LaAlO_3$ films at 650 °C in PLD. We sputtered four samples at various temperatures and 0.04 mbar for 25 min. The θ-2θ scans are shown in Fig. 3.1(d). The $LaAlO_3$ diffraction peak cannot be observed for the sample grown at 650 °C, while the sample grown at 700 °C shows a broad peak. Both samples are insulating. Clear $LaAlO_3$ peaks and interference fringes are visible for the samples grown at 750 °C and 800 °C. Both samples are conductive, which indicates that a higher growth temperature is necessary for the crystallization of the $LaAlO_3$ films.

3.3. Controlling conductivity by varying sputtering pressure

Having optimized the growth parameters, we now focus on the role of sputtering pressure in influencing the conductivity at the $LaAlO_3/SrTiO_3$ interface. We prepared five samples at 800 °C and various Ar pressures, ranging from 0.04 to 0.10 mbar (see Table 3.1). In the following the samples will be referred to with their growth pressure (sample 004 is grown at 0.04 mbar). Surface topologies were measured by tapping mode AFM. Epitaxial qualities of the interfaces were characterized by scanning transmission electron microscopy (STEM). Film thicknesses and lattice constants were determined by HRXRD. Magnetrotransport properties were measured in the PPMS by the van der Pauw method. Ohmic contacts were formed by wedge bonding Al wire directly to the sample surface.

3.3.1. Surface and interface

Fig. 3.2(a)-(e) show the AFM topographic images of the five samples. Atomically flat surfaces with clear step-and-terrace structures can be observed. The insets show the step height which corresponds to the $SrTiO_3$ (001) interplanar distance (≈ 3.905 Å).

Table 3.1: Growth pressure, in-plane lattice constant (a_{LAO}), out-of-plane lattice constant (c_{LAO}), thickness (t_{LAO}), deposition time, deposition rate and La/Al ratio of $LaAlO_3$ films. a_{LAO} was determined from the reciprocal space map. c_{LAO} and t_{LAO} were determined by fitting the θ-2θ scan. The deposition rate was calculated from the film thickness and the deposition time. The La/Al ratio was determined by interpolating c_{LAO} using the published results in Ref. [119].

Growth Pressure (mbar)	a_{LAO} (Å)	c_{LAO} (Å)	t_{LAO} (u.c.)	Dep. time (min)	Dep. rate (Å/min)	La/Al ratio
0.04	3.905(2)	3.734	16	14.0	4.27	0.88
0.06	3.905(1)	3.739	15	14.0	4.01	0.89
0.08	3.905(1)	3.745	15	14.8	3.79	0.91
0.09	3.905(2)	3.751	14	15.2	3.46	0.94
0.10	3.905(3)	3.763	17	20.0	3.20	1.00

Epitaxial qualities of the films were further characterized by high-angle annular dark field STEM (HAADF-STEM). The HAADF-STEM images of samples 004 and 010 are shown in Fig. 3.3(a) and (b). Well ordered interfaces between the film and the substrate are clearly visible. Fig. 3.3(c) shows the STEM electron energy loss spectroscopy (STEM-EELS) analysis of samples 004 and 010. This concentration profile is obtained by integration of the EELS intensity of the La-$M_{4,5}$ and Ti-$L_{2,3}$ edges during a spectrum image unit cell by unit cell in the growth direction. The profile is normalized by the maximum of intensity and cation vacancies are neglected. Identical intermixing (4 unit cells) was observed for both samples. This demonstrates that interdiffusion is a phenomenon that is not influenced by the growth pressure of the film.

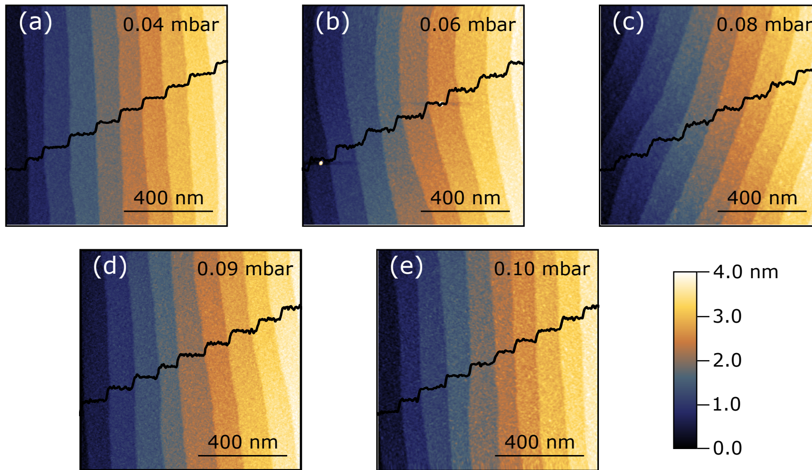

Figure 3.2: AFM topographic images of samples (a) 004, (b) 006, (c) 008, (d) 009 and (e) 010, using color code for the height. Insets are the height profiles of the surfaces.

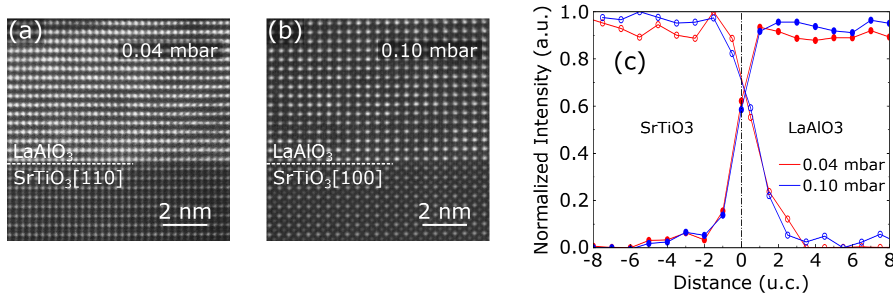

Figure 3.3: High-angle annular dark field STEM (HAADF-STEM) images of (a) sample 004 taken along the [110] direction and (b) sample 010 taken along the [100] direction. (c) STEM electron energy loss spectroscopy (STEM-EELS) analysis of samples 004 and 010, the La-$M_{4,5}$ (solid circles) and Ti-$L_{2,3}$ (open circles) edges integrated unit cell by unit cell across the interface. The data were acquired by D. Krishnan and N. Gauquelin at the University of Antwerp.

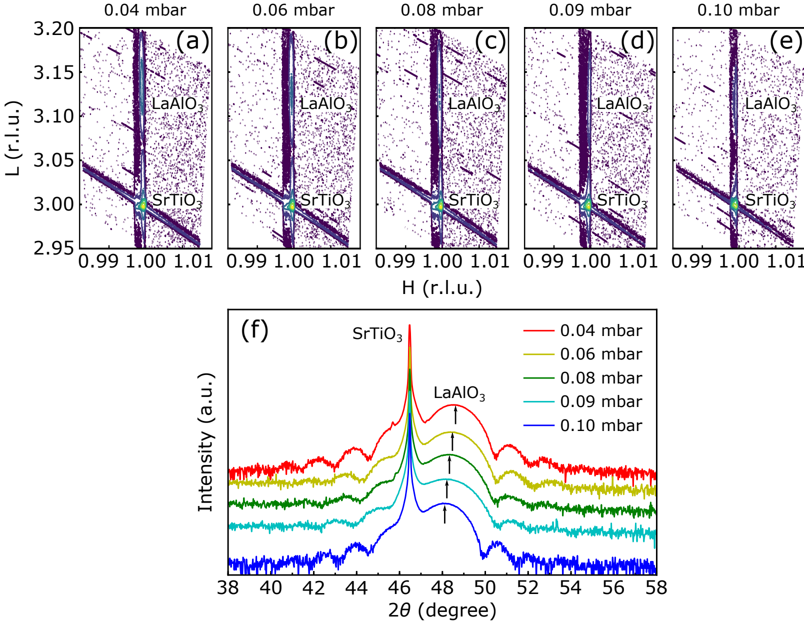

Figure 3.4: Reciprocal space maps (RSM) around the $SrTiO_3$ (103) diffraction peak of samples (a) 004, (b) 006, (c) 008, (d) 009 and (e) 010. (f) The θ-2θ scans for samples grown at various Ar pressures. The black arrows are the $LaAlO_3$ (002) diffraction peaks.

3.3.2. X-ray diffraction

Fig. 3.4(a)-(e) show the reciprocal space maps (RSM) around the $SrTiO_3$ (103) diffraction peak of the five samples. The films are coherently strained to the substrates, which means that the in-plane lattice constants (a_{LAO}) are ~ 3.905 Å. Fig. 3.4(f) shows the θ-2θ scans. The black arrows are the positions of the $LaAlO_3$ (002) diffraction peaks. It can be seen that as the sputtering pressure increases, the $LaAlO_3$ peak shifts to lower angle, which corresponds to an increase of the out-of-plane lattice constant (c_{LAO}) [119]. We extract c_{LAO} as well as the film thickness (t_{LAO}) by fitting the θ-2θ scans. Table 3.1 summarizes the estimated values for a_{LAO}, c_{LAO}, t_{LAO} and the deposition rate of the five samples. It has been reported that the increase of c_{LAO} is due to the increase of the La/Al ratio in $LaAlO_3$ films. The relationship between them was systematically studied by Qiao *et al.* [119]. Thus, we obtain the La/Al ratios of our samples by interpolating our data points using their published results. The interpolated La/Al ratios are listed in Table 3.1. As the sputtering pressure increases from 0.04 to 0.10 mbar, the La/Al ratio increases from 0.88 to 1.00.

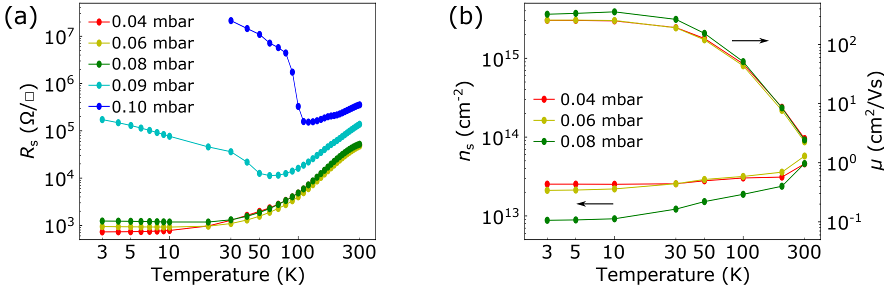

Figure 3.5: Temperature dependence of (a) the sheet resistance (R_S) and (b) the carrier density (n_S) and mobility (μ) for samples grown at various Ar pressures.

3

3.3.3. Transport properties

Fig. 3.5(a) shows the sheet resistance (R_S) as a function of temperature for samples grown at various Ar pressures. Samples 004, 006 and 008 show similar metallic behavior from 300 K to 3 K. The interfacial conductivity changes dramatically as the sputtering pressure further increases. For sample 009, R_S decreases from 1.4×10^5 Ω/□ at 300 K to 1.1×10^4 Ω/□ at 60 K and then gradually increases to 2.2×10^5 Ω/□ at 3 K. For sample 010, R_S decreases from 3.5×10^5 Ω/□ at 300 K to 1.6×10^5 Ω/□ at 100 K and abruptly changes to insulating state afterwards. The temperature dependence of the carrier density (n_S) and mobility (μ) for the metallic samples are shown in Fig. 3.5(b), which are determined by

$$n_S = \frac{B}{eR_{\text{Hall}}} \quad \text{and} \quad \mu = \frac{R_{\text{Hall}}}{BR_S(B=0)}. \tag{3.1}$$

The values of n_S and μ are approximately 1×10^{13} cm^{-2} and 2.6×10^2 cm^2/Vs at 3 K, respectively, which are consistent with reported results of the $LaAlO_3/SrTiO_3$ interfaces grown by sputtering [103] and PLD [41, 46].

3.4. Discussion

Our observations are consistent with the results reported by Warusawithana *et al.* [59], namely only Al-rich $LaAlO_3$ gives rise to a conductive interface. All of our $LaAlO_3$ films are epitaxially strained to the $SrTiO_3$ substrates. Increasing the sputtering pressure only increases the La/Al ratio, which we believe is due to light Al being scattered more easily at higher pressures [54, 57]. The dramatic change in the transport properties is related to the change of cation stoichiometry of the $LaAlO_3$ films. For the $LaAlO_3/SrTiO_3$ samples grown by PLD, it has also been reported that a slight variation in growth parameters modifies the cation stoichiometry of $LaAlO_3$ [54–56], resulting in a dramatic change in the interfacial conductivity. But the cation stoichiometry is not checked on a routine

basis. It may explain the fact that samples from different PLD groups are often hardly comparable, although similar growth parameters are used.

Our results help to gain some insights into the origin of the 2DES. First, it is well known that La-doped $SrTiO_3$ shows metallic behavior [120]. At the $LaAlO_3/SrTiO_3$ interface, La/Sr intermixing could be induced in two ways. One way is simply by the PLD process itself, during which the $SrTiO_3$ substrate is bombarded by particles with kinetic energies around several tens of eV [32]. In our off-axis sputtering deposition, we use relatively high Ar pressures (0.04-0.10 mbar), which correspond to mean free paths of several millimeters. The direct distance between the center of the target and the substrate is about 87.5 mm. The ejected particles would undergo multiple scatterings to slow down their speed before they deposit on the substrate. In our case, the chance of introducing La/Sr intermixing by high energy particle bombarding should be low. The other way is the dipole compensation mechanism proposed by Nakagawa *et al.* [23], where a compensating dipole is produced by La/Sr intermixing to reduce the interface dipole energy. We observed identical intermixing in samples 004 and 010. However, the intermixing does not appear to be crucial to the origin of conductivity. Otherwise the two samples would show similar conductive behavior.

Next, we discuss other possible mechanisms for the interfacial conductivity. Based on DFT calculations, Warusawithana *et al.* [59] concluded that the driver of conductivity is electronic reconstruction. However, it cannot be reconciled with the experimental observation that stoichiometric $LaAlO_3$ films grown by MBE and sputtering give rise to insulating interfaces. The fact that conductivity is only observed in Al-rich films may point to the oxygen vacancies being the doping mechanism. In this scenario, the excess Al in Al-rich films getter oxygen from $SrTiO_3$, which becomes n-type doped. Here we note that our samples grown in a mixture of Ar and O_2 show an insulating behavior. We suggest that the oxygen leads to oxidation of Al during the propagation towards the substrate [121], so that the Al is passivated and oxygen vacancies are not formed. The limited conductivity in stoichiometric $LaAlO_3$ films grown by PLD [54] can similarly be explained by defect generation induced by energetic particles in the ablation plume. On the other hand, we also observed that a conducting amorphous $LaAlO_3/SrTiO_3$ sample became insulating after post annealing in oxygen. This would indicate that the annealing treatment is efficient enough to remove the oxygen vacancies which are formed by the redox reaction [36]. It is therefore still not fully clear whether the observed conductivity in Al-rich samples is completely dominated by the oxygen vacancies formed in $SrTiO_3$, but our observations on sputtered interfaces give good reasons to believe that the formation of oxygen vacancies is an important part of the puzzle.

3.5. Conclusion

In summary, high quality epitaxial $LaAlO_3$ films were grown on $SrTiO_3$ (001) substrates by 90° off-axis sputtering. While increasing the growth pressure, little structural variations have been observed, except for an increase of the out-of-plane lattice constant, which indicates an increase of the La/Al ratio. Metallic conductive interfaces were only found in Al-rich samples. Our results emphasize that cation stoichiometry in $LaAlO_3$ films plays an important role in the formation of interfacial conductivity at the $LaAlO_3/SrTiO_3$ interfaces.